Progress In Electromagnetics Research, PIER 60, 1–18, 2006

OPTIMIZATION APPROACH TO THE RETRIEVAL OF THE CONSTITUTIVE PARAMETERS OF A SLAB OF GENERAL BIANISOTROPIC MEDIUM

X. Chen

Department of Electrical & Computer Engineering
National University of Singapore
4 Engineering Dr. 3, E4-05-48, Singapore 117576

T. M. Grzegorczyk and J. A. Kong

Research Laboratory of Electronics
Massachusetts Institute of Technology
77 Mass. Av., 26-305, Cambridge, MA 02139, USA

Abstract—The reconstruction of the frequency-dispersive constitutive parameters of general bianisotropic media is achieved by an optimization approach. The constitutive parameters are optimized in order to match the measured reflection and transmission data for plane wave incidence onto bianisotropic slabs. Two optimization methods, in our case the differential evolution (DE) algorithm and the Nelder-Mead simplex method, are used for the reconstruction at low frequencies. The Nelder-Mead simplex method is then used to obtain the solutions at higher frequencies, where the initial guess is obtained by the linear extrapolation of the solutions at previous frequencies. The proposed reconstruction method is tested with both noiseless and noisy data, and is proven feasible and robust.

1. INTRODUCTION

Left-handed metamaterials have been a subject of important scientific interest since the first experimental verification of a negative refraction. Both theoretical and experimental results show that not only isotropic media with simultaneously negative permittivity and permeability achieve a negative refraction, but also anisotropic and bianisotropic media. The refraction diagram of biaxial media where the diagonal constitutive parameters can take negative values is proposed in [1],

and a generalization of Snell's law to this situation is proposed in [2]. Going beyond biaxial media, [3] shows that bianisotropy is an important parameter for exhibiting negative refraction.

Constitutive parameters are important in quantitatively characterizing the wave propagation inside metamaterials [4, 5], but they are usually unknown to us. As stated in [6], the retrieval method from the reflection and transmission data is the prime approach to obtain these constitutive parameters. While there are many approaches to retrieve the isotropic parameters [7, 8], only [9] deals with the retrieval of the bianisotropic parameters. It should be noted, however, that in [9], the cross-polarization properties of the medium are known a priori. For more complicated metamaterial structures, the cross-polarization properties remain unknown and a more general retrieval method is needed.

This paper presents a method to retrieve the constitutive parameters of a general bianisotropic slab from the knowledge of the reflection and transmission matrix via an optimization approach. Each of the permittivity tensor ($\overline{\overline{\epsilon}}$), permeability tensor ($\overline{\overline{\mu}}$), and cross-polarization tensors ($\overline{\overline{\xi}}$, $\overline{\overline{\zeta}}$) is a three by three matrix with complex elements, so that there is a total of 72 parameters to be retrieved. The retrieval method of obtaining the 72 parameters of a homogeneous slab was developed by G. N. Borzdov in [10, 11], where the slabs with different values of thickness and cuts were illuminated by plane waves at a certain frequency. However, the requirement of having slabs of different thicknesses and cuts cannot always be satisfied in practice. In this scenario, we need to resort to an optimization approach. In this paper, differential evolution (DE) and Nelder-Mead simplex optimization methods are used in order to obtain the global-minimum solution. In the optimization, we minimize the relative mismatch between the measured reflection/transmission data and the calculated ones from the forward approach, where the reflection and transmission coefficients for a plane wave obliquely or normally incident upon a slab in free space are calculated by the notion of propagators and wave-splitting technique [12].

In our numerical validation, we first apply our method to the retrieval of a rotated omega medium, where 17 parameters need to be optimized. Then, we apply the proposed method to the retrieval of two general bianisotropic media, where 72 parameters are optimized. In all cases, we obtain a group of solutions, instead of a single solution, which shows the robustness of the proposed optimization method.

2. PROBLEM FORMULATION AND FORWARD APPROACH

Consider a time-harmonic electromagnetic plane wave obliquely (or normally) impinging from the region $z < 0$ onto a homogeneous slab located in the region $z \in [0, d]$. Both sides of the slab are free space. The incident wave vector $\overline{k}_i$ is expressed as $\overline{k}_i = (\hat{x}\sin\theta\cos\phi + \hat{y}\sin\theta\sin\phi + \hat{z}\cos\theta)k_0$, where $\theta \in [0, \pi/2]$ and ϕ are the polar and azimuthal angle of the incident wave, respectively, and k_0 denotes the wavenumber in free space. The homogeneous slab is characterized by the electromagnetic parameters $\overline{\overline{\epsilon}}$, $\overline{\overline{\mu}}$, $\overline{\overline{\xi}}$, and $\overline{\overline{\zeta}}$, and its constitutive relationships are

$$\overline{D} = \overline{\overline{\epsilon}} \cdot \overline{E} + \overline{\overline{\xi}} \cdot \overline{H}, \tag{1}$$

$$\overline{B} = \overline{\overline{\mu}} \cdot \overline{H} + \overline{\overline{\zeta}} \cdot \overline{E}. \tag{2}$$

In the forward problem, the reflection and transmission coefficients are calculated by the notion of propagators and wave-splitting technique [12]. Inside the slab, the tangential electric and magnetic fields satisfy the following equations,

$$\frac{d}{dz}\begin{pmatrix} \overline{E}_{xy}(z) \\ \eta_0\overline{\overline{J}} \cdot \overline{H}_{xy}(z) \end{pmatrix} = ik_0\overline{\overline{M}} \cdot \begin{pmatrix} \overline{E}_{xy}(z) \\ \eta_0\overline{\overline{J}} \cdot \overline{H}_{xy}(z) \end{pmatrix} \tag{3}$$

where $\overline{\overline{J}}$ is a two-dimensional rotation dyadic, and $\overline{\overline{M}}$, a function of $\overline{\overline{\epsilon}}$, $\overline{\overline{\mu}}$, $\overline{\overline{\xi}}$, and $\overline{\overline{\zeta}}$, is the fundamental dyad of the bianisotropic medium whose explicit expression can be found in [12]. Upon integrating, we map the fields on the left-hand side boundary ($z = 0$) to the right-hand side boundary ($z = d$) as

$$\begin{pmatrix} \overline{E}_{xy}(d) \\ \eta_0\overline{\overline{J}} \cdot \overline{H}_{xy}(d) \end{pmatrix} = \overline{\overline{P}} \cdot \begin{pmatrix} \overline{E}_{xy}(0) \\ \eta_0\overline{\overline{J}} \cdot \overline{H}_{xy}(0) \end{pmatrix} \tag{4}$$

where $\overline{\overline{P}} = e^{ik_0 d\overline{\overline{M}}}$ is known as the propagator. On both sides of the slab, the wave splitting technique is used in free space,

$$\begin{cases} \overline{E}_{xy}(z) = \overline{E}^{+}(z) + \overline{E}^{-}(z) \\ \eta\overline{\overline{J}} \cdot \overline{H}_{xy}(z) = -\overline{\overline{O}}^{-1} \cdot \overline{E}^{+}(z) + \overline{\overline{O}}^{-1} \cdot \overline{E}^{-}(z) \end{cases} \tag{5}$$

where $\overline{\overline{O}}$ is assimilated to an impedance dyad [12]. By combining Eqs. (4) and (5), we obtain the scattering relation,

$$\begin{pmatrix} \overline{E}^{+}(d) \\ \overline{E}^{-}(d) \end{pmatrix} = \overline{\overline{T}} \cdot \begin{pmatrix} \overline{E}^{+}(0) \\ \overline{E}^{-}(0) \end{pmatrix}. \tag{6}$$

The reflection and transmission dyads for the tangential electric field are defined by

$$\begin{cases} \overline{\overline{r}} = -\overline{\overline{T}}_{22}^{-1} \cdot \overline{\overline{T}}_{21} \\ \overline{\overline{t}} = \overline{\overline{T}}_{11} + \overline{\overline{T}}_{12} \cdot \overline{\overline{r}} \end{cases} \tag{7}$$

In terms of the strengths of the fields of TE and TM waves, the reflection and transmission coefficients are defined to be

$$r_{EE} = r_{22},\ r_{EM} = r_{21}\cos\theta,\ r_{ME} = -r_{12}/\cos\theta,\ r_{MM} = -r_{11} \tag{8}$$

$$t_{EE} = t_{22},\ t_{EM} = t_{21}\cos\theta,\ t_{ME} = t_{12}/\cos\theta,\ t_{MM} = t_{11} \tag{9}$$

and the reflection and transmission tensors in terms of the fields strengths are

$$\overline{\overline{r}} = \begin{pmatrix} r_{EE} & r_{EM} \\ r_{ME} & r_{MM} \end{pmatrix}, \quad \overline{\overline{t}} = \begin{pmatrix} t_{EE} & t_{EM} \\ t_{ME} & t_{MM} \end{pmatrix} \tag{10}$$

The aforementioned method have been compared with the one presented in [3] for a variety of numerical cases. In all of them, the two methods yielded identical results, validating in this way the forward method used in this paper.

3. OPTIMIZATION APPROACH TO INVERSE PROBLEM

3.1. Objective Function

In the inverse problem, we optimize the constitutive parameters so that the calculated reflection and transmission data match the measured ones. We denote all the parameters to be optimized by $\overline{x}$, and define the objective function as,

$$\begin{aligned} f(\overline{x}) = \sum_{\{\theta,\phi\}} \sum_{i,j\in\{1,2\}} \Big\{ & W_{ij}^r(\theta,\phi)|\tilde{r}_{ij}(\theta,\phi) - \tilde{r}_{ij}^m(\theta,\phi)|^2 \\ & + W_{ij}^t(\theta,\phi)|\tilde{t}_{ij}(\theta,\phi) - \tilde{t}_{ij}^m(\theta,\phi)|^2 \Big\} \end{aligned} \tag{11}$$

where $\tilde{r}_{ij}(\theta,\phi), \tilde{t}_{ij}(\theta,\phi)$ are the calculated reflection and transmission coefficients, and $\tilde{r}_{ij}^m(\theta,\phi), \tilde{t}_{ij}^m(\theta,\phi)$ are the measured ones. The weighting factor is chosen as $W_{ij}^r(\theta,\phi) = 1/(|\tilde{r}_{ij}^m(\theta,\phi)|+\alpha)$, where α is a positive parameter that avoids an infinite weight for small magnitudes of $\tilde{r}_{ij}^m(\theta,\phi)$. Note that W_{ij}^t is defined similarly.

The optimization method seeks at minimizing the objective function whose global-minimum value is zero, which is obtained when the measured and computed data are identical, indicating that the retrieved constitutive tensors are identical to the original ones.

3.2. Optimization Methods

The optimization problem Eq. (11) is highly non-linear, since all the unknown parameters are in the argument of the exponential function in Eq. (4). The objective function has many local minima, which makes the search for a global minimum intractable with deterministic optimization methods. Hence stochastic optimization methods should be used instead. However, stochastic methods are often slowly-convergent. Therefore, we design here a hybrid optimization algorithm, which combines the DE [13] algorithm to the simplex method.

Differential evolution algorithm is a stochastic parallel direct search optimization algorithm, which utilizes a number of parameter vectors, known as individuals, as a generation to explore the search space. In each generation, mutation and crossover operators are applied to the individuals of the current generation to generate a trial population. The corresponding individuals in the two populations compete in the selection operation to become members of the next generation. The mutation operator of DE generates new parameter vectors by adding the weighted difference between two parameter vectors to a third one. The algorithm stops when a specified maximum number of generations is reached. Numerical simulations show the DE algorithm exhibits good global searching ability [13].

Simplex method [14] is a direct search optimization algorithm, i.e., there is no need for gradient information of the objective function. The geometric figure formed by a set of $n+1$ points in an n-dimensional space is called a simplex. The basic idea of simplex optimization method is to compare the values of the objective function at the $n+1$ vertices of a simplex and rearrange the simplex gradually toward the optimum point during the iterative process. The movement of the simplex is achieved by using three operations: reflection, contractions, and expansion. The movement stops when the standard deviation of the function at the $n+1$ vertices of the simplex is smaller than a prescribed small quantity. Simplex method is good at searching local minima and converges fast compared to the DE algorithm.

In the retrieval of bianisotropy media, DE is first used to perform a parallel search in order to explore the entire solution space, and yields a set of solutions bearing good genes. The simplex method, which is good at obtaining local minimum, is used subsequently, taking the solution set from the DE as initial guesses.

4. NUMERICAL RECONSTRUCTION

In this section, numerical examples are presented to show the feasibility and the robustness of the proposed optimization method. In the first

example, a priori properties of the medium are known so that the total number of unknowns is reduced. In the subsequent examples, we apply a 72-parameter retrieval method to two arbitrarily chosen media. In all cases, we show that the proposed method is able to reconstruct the constitutive tensors despite the high nonlinearity of the problem. Note that in all numerical examples, we first calculate the reflection and transmission parameters using the forward problem solver, and then treat them as the measured ones to evaluate the optimized ones in the inverse process.

4.1. Rotated Omega Medium

In this first example, prior knowledge of the medium is assumed: we know that the medium to be retrieved is an Omega medium, yet, the numerical values of the constitutive parameters and the axes of the medium are unknown. Hence, we characterize the medium through the tensors,

$$\begin{aligned}
\overline{\overline{\epsilon}} &= \epsilon_0 U^T \cdot \begin{pmatrix} \epsilon_x & 0 & 0 \\ 0 & \epsilon_y & 0 \\ 0 & 0 & \epsilon_z \end{pmatrix} \cdot U,\ \overline{\overline{\mu}} = \mu_0 U^T \cdot \begin{pmatrix} \mu_x & 0 & 0 \\ 0 & \mu_y & 0 \\ 0 & 0 & \mu_z \end{pmatrix} \cdot U, \\
\overline{\overline{\xi}} &= \frac{1}{c} U^T \cdot \begin{pmatrix} 0 & 0 & 0 \\ 0 & 0 & 0 \\ 0 & -i\xi_0 & 0 \end{pmatrix} \cdot U,\ \overline{\overline{\zeta}} = \frac{1}{c} U^T \cdot \begin{pmatrix} 0 & 0 & 0 \\ 0 & 0 & i\xi_0 \\ 0 & 0 & 0 \end{pmatrix} \cdot U, \quad (12)
\end{aligned}$$

where U is the rotation matrix defined by Euler angles (α, β, γ) [15]. Consequently, the optimization vector contains 17 unknowns, $\overline{x} = (\alpha, \beta, \gamma, \epsilon'_x, \epsilon'_y, \epsilon'_z, \epsilon''_x, \epsilon''_y, \epsilon''_z, \mu'_x, \mu'_y, \mu'_z, \mu''_x, \mu''_y, \mu''_z, \xi'_0, \xi''_0)$, where $(\cdot)'$ and $(\cdot)''$ denote the real part and imaginary part operators, respectively.

Various values and frequency dependent functions have been successfully retrieved with our method, although these are not shown here. For the sake of illustration, we choose here the following parameters,

$$\begin{aligned}
&\alpha = \pi/5 && \beta = \pi/4 && \gamma = \pi/6 \\
&\epsilon_x = 1 - \frac{F_{ex} f^2}{(f^2 - f_{ex}^2 + i\gamma_{ex} f)} && \epsilon_y = 1 - \frac{F_{ey} f^2}{(f^2 - f_{ey}^2 + i\gamma_{ey} f)} \\
&\epsilon_z = 1 - \frac{F_{ez} f^2}{(f^2 - f_{ez}^2 + i\gamma_{ez} f)} && \mu_x = 1 - \frac{F_{mx} f^2}{(f^2 - f_{mx}^2 + i\gamma_{mx} f)} \\
&\mu_y = 1 - \frac{F_{my} f^2}{(f^2 - f_{my}^2 + i\gamma_{my} f)} && \mu_z = 1 - \frac{F_{mz} f^2}{(f^2 - f_{mz}^2 + i\gamma_{mz} f)}
\end{aligned}$$

$$\xi_0 = 1 - \frac{F_\xi f^2}{(f^2 - f_\xi^2 + i\gamma_\xi f)} \tag{13}$$

where $f_{ex} = 4.0\,\text{GHz}$, $f_{ey} = 5.0\,\text{GHz}$, $f_{ez} = 3.5\,\text{GHz}$, $f_{mx} = 5.0\,\text{GHz}$, $f_{mx} = 4.0\,\text{GHz}$, $f_{mx} = 3.5\,\text{GHz}$, $f_\xi = 4.0\,\text{GHz}$, $\gamma_{ex} = 0.5\,\text{GHz}$, $\gamma_{ey} = 0.4\,\text{GHz}$, $\gamma_{ez} = 0.3\,\text{GHz}$, $\gamma_{mx} = 0.4\,\text{GHz}$, $\gamma_{my} = 0.3\,\text{GHz}$, $\gamma_{mz} = 0.2\,\text{GHz}$, $\gamma_\xi = 0.5\,\text{GHz}$, $F_{ex} = 0.5$, $F_{ey} = 0.3$, $F_{ez} = 0.4$ $F_{mx} = 0.3$, $F_{my} = 0.2$, $F_{mz} = 0.3$ and $F_\xi = 0.4$. The operating frequency range is from 2 GHz to 8 GHz and the thickness of the slab is $\lambda_0/20$, where λ_0 is the wavelength in free space at the initial frequency. The incident angles are chosen to be $(\theta, \phi) \in \{(45^\circ, 0^\circ), (45^\circ, 45^\circ), (45^\circ, 90^\circ)\}$.

For the initial frequency of 2 GHz, we use the DE and the simplex methods to optimize for the constitutive parameters and the rotation angles. In the first stage of the optimization, DE runs for 2000 generations, with a total population of 170 individuals in each generation. Subsequently, half of the population of the last generation is used in the simplex method, where each of the individuals is treated as an initial guess. After the first round of simplex method, about half of the solutions are chosen as initial guesses for the second round of simplex optimization. The above procedure is iterated until solutions

Table 1. Optimization results for the rotated Omega medium.

	Exact	Optimized 1st	Optimized 2nd	Optimized 3rd	Optimized 4th
α	6.2832e-01	6.2964e-01	6.2978e-01	6.2844e-01	3.7698e+00
β	7.8540e-01	7.8695e-01	7.8708e-01	7.8554e-01	2.3563e+00
γ	5.2360e-01	5.2271e-01	5.2259e-01	3.6651e+00	2.6179e+00
ϵ'_x	1.1655e+00	1.1651e+00	1.1650e+00	1.1654e+00	1.1655e+00
ϵ'_y	1.0571e+00	1.0571e+00	1.0571e+00	1.0571e+00	1.0571e+00
ϵ'_z	1.1929e+00	1.1936e+00	1.1936e+00	1.1928e+00	1.1929e+00
ϵ''_x	1.3793e-02	1.5862e-02	1.6209e-02	1.3972e-02	1.3662e-02
ϵ''_y	2.1737e-03	2.1362e-03	2.1529e-03	2.1664e-03	2.1756e-03
ϵ''_z	1.4030e-02	1.4184e-02	1.4285e-02	1.3988e-02	1.3987e-02
μ'_x	1.0571e+00	1.0570e+00	1.0570e+00	1.0571e+00	1.0571e+00
μ'_y	1.0665e+00	1.0660e+00	1.0662e+00	1.0665e+00	1.0665e+00
μ'_z	1.1451e+00	1.1446e+00	1.1448e+00	1.1451e+00	1.1451e+00
μ''_x	2.1737e-03	2.2299e-03	2.1899e-03	2.2087e-03	2.1763e-03
μ''_y	3.3250e-03	4.2892e-04	4.9731e-06	3.2113e-03	3.4997e-03
μ''_z	7.0358e-03	6.7278e-03	6.5528e-03	7.0260e-03	7.0613e-03
ξ'_0	1.1324e+00	1.1330e+00	1.1331e+00	-1.1324e+00	-1.1324e+00
ξ''_0	1.1034e-02	1.0586e-02	1.0560e-02	-1.1077e-02	-1.1043e-02
$f(\overline{x})$	0	2.5906e-05	2.8427e-05	3.7121e-06	1.6790e-06

with small objective functions are achieved. In the present numerical example, we obtain four solutions shown in Table 1 by using the DE and five rounds of simplex method. The fact that the coordinate axes are labeled differently (for example, the $\hat{x}$ and $\hat{y}$ are labeled as $-\hat{x}$ and $-\hat{y}$, respectively, in the third solution) makes the solutions seemingly different from each other. In fact, the four solutions are almost identical when expressed in the rotated form as in Eq. (12). For the retrieval at higher frequencies, we choose the linear extrapolation of the results at the previous two frequencies as the initial guess for the simplex optimization.

In order to quantitatively describe the match between the true and the retrieved constitutive parameters, we define the relative mismatch (RM) as

$$RM(\rho) = \begin{cases} \dfrac{|\rho_t - \rho_r|}{|\rho_t|} & \text{if } |\rho_t| > \tau, \\ |\rho_r| & \text{otherwise,} \end{cases} \tag{14}$$

where τ is a small positive parameter, ρ can be any component of constitutive tensors, and the subscripts "t" and "r" denote "true" and "retrieved", respectively. In numerical examples, we choose τ to be 0.05. To represent the mismatch across all sample frequencies, we define an averaged relative mismatch (A_{RM}) to be the mean of RM across all sample frequencies.

The optimization results show that the true and the optimized results are almost identical at most frequencies for the components of $\overline{\overline{\epsilon}}$, $\overline{\overline{\mu}}$, and $\overline{\overline{\xi}}$. Here only ξ_0 is shown in Fig. 1 for the purpose of illustration. The maximum A_{RM} among the seven components is obtained on ξ_0, and amounts to 0.0096.

4.2. General Bianisotropic Medium

In the following two numerical examples, we consider the problem of parameter reconstruction in media with arbitrary constitutive parameters. In the forward problem, we consider two media, known as Chiroferrite $D_\infty(C_\infty)$ and Omegaferrite $C_{2v}(C_s)$ [16].

The constitutive tensors of the Chiroferrite $D_\infty(C_\infty)$ is given by

$$\begin{aligned} \overline{\overline{\epsilon}} &= \epsilon_0 \begin{pmatrix} \epsilon_{xx} & \epsilon_{xy} & 0 \\ -\epsilon_{xy} & \epsilon_{xx} & 0 \\ 0 & 0 & \epsilon_{zz} \end{pmatrix}, \ \overline{\overline{\mu}} = \mu_0 \begin{pmatrix} \mu_{xx} & \mu_{xy} & 0 \\ -\mu_{xy} & \mu_{xx} & 0 \\ 0 & 0 & \mu_{zz} \end{pmatrix}, \\ \overline{\overline{\xi}} &= \frac{1}{c} \begin{pmatrix} \xi_{xx} & \xi_{xy} & 0 \\ -\xi_{xy} & \xi_{xx} & 0 \\ 0 & 0 & \xi_{zz} \end{pmatrix}, \ \overline{\overline{\zeta}} = \frac{1}{c} \begin{pmatrix} -\xi_{xx} & -\xi_{xy} & 0 \\ \xi_{xy} & -\xi_{xx} & 0 \\ 0 & 0 & -\xi_{zz} \end{pmatrix}. \end{aligned} \tag{15}$$

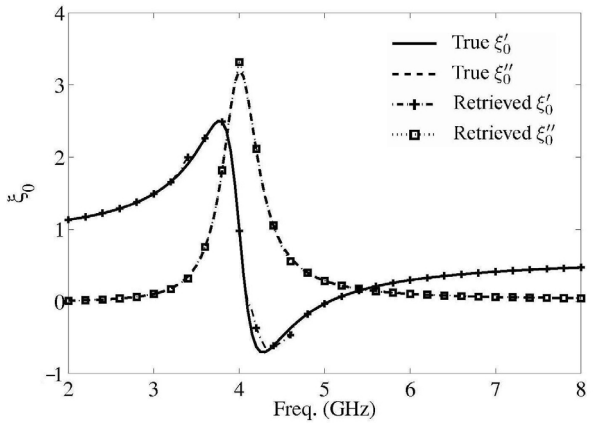

Figure 1. Comparison of the retrieved and the true ξ_0 of an Omega medium.

It is important to highlight that although the tensors have some zero components, this is not an information used by our method and we optimize 72 parameters, thus retrieving a value of zero whenever necessary. The non-zero parameters are chosen to be

$$\begin{aligned}
\epsilon_{xx} &= 1 - \frac{f_{pexx}^2}{(f^2 - f_{0exx}^2 + i\gamma_{exx} f)} \qquad \epsilon_{xy} = 0.1 + 0.05i \\
\epsilon_{zz} &= 1 - \frac{f_{pezz}^2}{(f^2 - f_{0ezz}^2 + i\gamma_{ezz} f)} \qquad \mu_{xx} = 1 - \frac{f_{pmxx}^2}{(f^2 - f_{0mxx}^2 + i\gamma_{mxx} f)} \\
\mu_{xy} &= 0.1i \quad \mu_{zz} = 1 \\
\xi_{xx} &= 1 - e^{-f/10^{10}} \qquad \xi_{xy} = 1 - \frac{f_{p\xi}^2}{(f^2 - f_{0\xi}^2 + i\gamma_{\xi} f)} \\
\xi_{zz} &= (0.1 + 0.05i) f/10^9
\end{aligned} \tag{16}$$

with $f_{pexx} = 4.5\,\text{GHz}$, $f_{pezz} = 3.5\,\text{GHz}$, $f_{pmxx} = 4.0\,\text{GHz}$, $f_{p\xi} = 3.0\,\text{GHz}$, $f_{0exx} = 4.0\,\text{GHz}$, $f_{0ezz} = 3.0\,\text{GHz}$, $f_{0mxx} = 3.5\,\text{GHz}$, $f_{0\xi} = 2.5\,\text{GHz}$, $\gamma_{exx} = 2.0\,\text{GHz}$, $\gamma_{ezz} = 1.2\,\text{GHz}$, $\gamma_{mxx} = 1.5\,\text{GHz}$, and $\gamma_{\xi} = 1.1\,\text{GHz}$. We first optimize the parameters at the initial frequency of 0.1 GHz. Totally unconstrained optimization problems with 72 unknowns are difficult and time-consuming to deal with, so we resort to a physical assumption that simplifies the optimization problem and makes it manageable on a single PC within a few hours. Our assumption is that the bianisotropy is weak, namely, $\overline{\overline{\xi}}$ and $\overline{\overline{\zeta}}$ approach zero at relatively low frequencies, which is true for most

materials. Hence, at the first stage of the optimization, $\overline{\overline{\epsilon}}$ and $\overline{\overline{\mu}}$ are optimized with $\overline{\overline{\xi}}$ and $\overline{\overline{\zeta}}$ being zero. When a good match in reflection and transmission is achieved, *i.e.*, $\overline{\overline{\epsilon}}$ and $\overline{\overline{\mu}}$ are close to the exact solution, we start the second-stage of optimization, where $\overline{\overline{\xi}}$ and $\overline{\overline{\zeta}}$, together with $\overline{\overline{\epsilon}}$ and $\overline{\overline{\mu}}$ are optimized at low frequencies, with the solution obtained at the first stage serving as the initial guess.

In the numerical simulation, we take a slab thickness of $\lambda_0/30$, where λ_0 denotes the wavelength in free space at the initial frequency (0.1 GHz). Note also the importance of the thickness of the slab in the optimization: if the slab is too thin compared with the wavelength, it is almost transparent so that the reflection is almost zero and the transmission is almost unity. On the other hand, if the slab is too thick, the problem becomes dramatically nonlinear and is difficult to optimize. From our experience, thicknesses within $\lambda_0/30$ to $\lambda_0/10$ are good for the optimization at the initial frequency.

There are two important issues in solving the inverse problem with 72 parameters, namely uniqueness and computational burden. Fewer incidences are likely to result in non-uniqueness, while too many incidences require intractable computation power. Therefore, it would be valuable to know the number of the incidence directions that are necessary and sufficient to obtain a unique solution with a manageable computational burden. Unfortunately, it is difficult or even impossible to answer this question and we have to choose the incidence directions empirically. In our numerical simulations, we choose different number of incidences at different optimization stages. Since the DE algorithm explores the search space using a group of individuals as a generation, it is characterized by the properties of good global searching abilities but also is time-consuming. In this respect, we choose few incidences in the DE optimization. On the other hand, since there are fewer individuals in the simplex method and we aim at obtaining the unique solution at this optimization stage, we choose more incidences in the simplex optimization.

At the first stage of the optimization, *i.e.*, looking for $\overline{\overline{\epsilon}}$ and $\overline{\overline{\mu}}$ with $\overline{\overline{\xi}}$ and $\overline{\overline{\zeta}}$ being zero, the DE is applied first and the simplex method is used subsequently. In the DE optimization, the slab is illuminated at normal incidence as well as oblique incidences with $\theta = \frac{4\pi}{9}$ and seven ϕ evenly distributed from 0 to 2π, which is shorted as $< \frac{4\pi}{9}, 7 >$. The population in each generation is 360 and the total generation of the evolution is 2000. Subsequently, the simplex method is used to realize the local search, where more incidences ($< \frac{2\pi}{5}, 5 >$, $< \frac{\pi}{3}, 4 >$) are added in addition to the original ones. Simplex method is sequentially carried out until there is no significant improvement over the results

obtained from the previous round. We finally obtain 6 solutions, all of which have an objective function smaller than 0.003.

At the second stage of the optimization, we use the results obtained at the first stage as initial guesses, and optimize 72 constitutive parameters to further match the reflection and transmission coefficients. During the sequential application of the simplex method, we drop the worst one among the 6 solutions due to its slow convergence, and finally obtain 5 solutions, all of which are close to the exact solution. The best one $\overline{x}_{opt}$, with the objective function value 8.2819×10^{-5}, is expressed in tensor form as

$$\overline{\overline{\epsilon}} = \begin{pmatrix} 2.25 \times 10^0 + i3.11 \times 10^{-2} & 1.00 \times 10^{-1} + i5.01 \times 10^{-2} & -1.73 \times 10^{-3} - i1.35 \times 10^{-3} \\ -1.00 \times 10^{-1} - i5.00 \times 10^{-2} & 2.25 \times 10^0 + i3.10 \times 10^{-2} & 2.05 \times 10^{-3} - i1.64 \times 10^{-3} \\ -1.64 \times 10^{-3} - i1.30 \times 10^{-3} & -1.07 \times 10^{-3} - i1.14 \times 10^{-3} & 2.42 \times 10^0 - i5.96 \times 10^{-2} \end{pmatrix},$$

$$\overline{\overline{\mu}} = \begin{pmatrix} 2.29 \times 10^0 + i2.99 \times 10^{-2} & -7.05 \times 10^{-5} + i1.00 \times 10^{-1} & -6.17 \times 10^{-4} - i5.27 \times 10^{-4} \\ 2.96 \times 10^{-5} - i1.00 \times 10^{-1} & 2.29 \times 10^0 + i2.99 \times 10^{-2} & -3.77 \times 10^{-4} - i5.25 \times 10^{-4} \\ -7.62 \times 10^{-4} - i5.63 \times 10^{-4} & 8.60 \times 10^{-4} - i7.34 \times 10^{-4} & 1.01 \times 10^0 - i1.47 \times 10^{-2} \end{pmatrix},$$

$$\overline{\overline{\xi}} = \begin{pmatrix} 9.68 \times 10^{-3} + i4.91 \times 10^{-5} & 2.53 \times 10^{-3} + i1.83 \times 10^{-2} & -4.38 \times 10^{-5} + i3.23 \times 10^{-5} \\ -2.55 \times 10^{-3} - i1.83 \times 10^{-2} & 9.68 \times 10^{-3} + i1.99 \times 10^{-5} & 1.14 \times 10^{-5} + i1.62 \times 10^{-5} \\ -6.77 \times 10^{-4} + i1.12 \times 10^{-4} & 3.81 \times 10^{-4} + i4.03 \times 10^{-4} & 1.06 \times 10^{-2} + i4.37 \times 10^{-3} \end{pmatrix},$$

$$\overline{\overline{\zeta}} = \begin{pmatrix} -9.96 \times 10^{-3} + i - 1.42 \times 10^{-4} & -3.02 \times 10^{-3} - i1.97 \times 10^{-2} & 7.83 \times 10^{-5} + i3.38 \times 10^{-5} \\ 3.03 \times 10^{-3} + i1.97 \times 10^{-2} & -9.96 \times 10^{-3} - i1.28 \times 10^{-4} & 9.58 \times 10^{-5} + i3.37 \times 10^{-5} \\ -1.04 \times 10^{-4} + i1.35 \times 10^{-4} & -1.48 \times 10^{-4} - i6.82 \times 10^{-5} & -1.13 \times 10^{-2} - i4.65 \times 10^{-3} \end{pmatrix}.$$

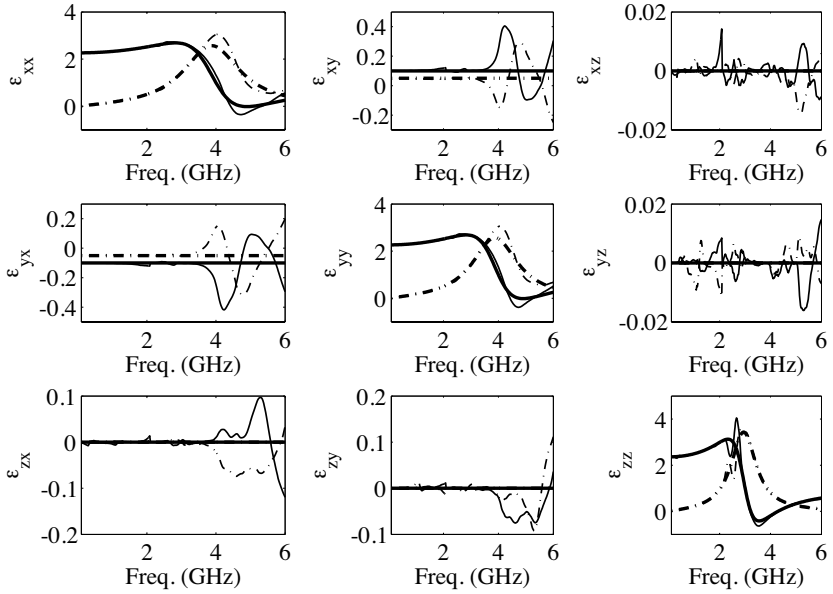

Figure 2. Comparison of the retrieved (thin lines) and the true (thick lines) $\overline{\overline{\epsilon}}$ of a Chiroferrite medium. The solid and dotted-dashed lines are for the real and imaginary parts, respectively.

We find that the solution is fairly close to the true solution $\overline{x}_t$:

$$\overline{\overline{\epsilon}}_t = \begin{pmatrix} 2.26 \times 10^0 + i1.58 \times 10^{-2} & 1.00 \times 10^{-1} + i5.00 \times 10^{-2} & 0 \\ -1.00 \times 10^{-1} - i5.00 \times 10^{-2} & 2.26 \times 10^0 + i1.58 \times 10^{-2} & 0 \\ 0 & 0 & 2.36 \times 10^0 + i1.81 \times 10^{-2} \end{pmatrix},$$

$$\overline{\overline{\mu}}_t = \begin{pmatrix} 2.30\times10^0+i1.60\times10^{-2} & i1.00 \times 10^{-1} & 0 \\ -i1.00 \times 10^{-1} & 2.30\times10^0+i1.60\times10^{-2} & 0 \\ 0 & 0 & 1.00\times10^0 \end{pmatrix},$$

$$\overline{\overline{\xi}}_t = \begin{pmatrix} 9.95 \times 10^{-3} & 1.85 \times 10^{-3} + i2.54 \times 10^{-2} & 0 \\ -1.85 \times 10^{-3} - i2.54 \times 10^{-2} & 9.95 \times 10^{-3} & 0 \\ 0 & 0 & 1.00 \times 10^{-2} + i5.00 \times 10^{-3} \end{pmatrix},$$

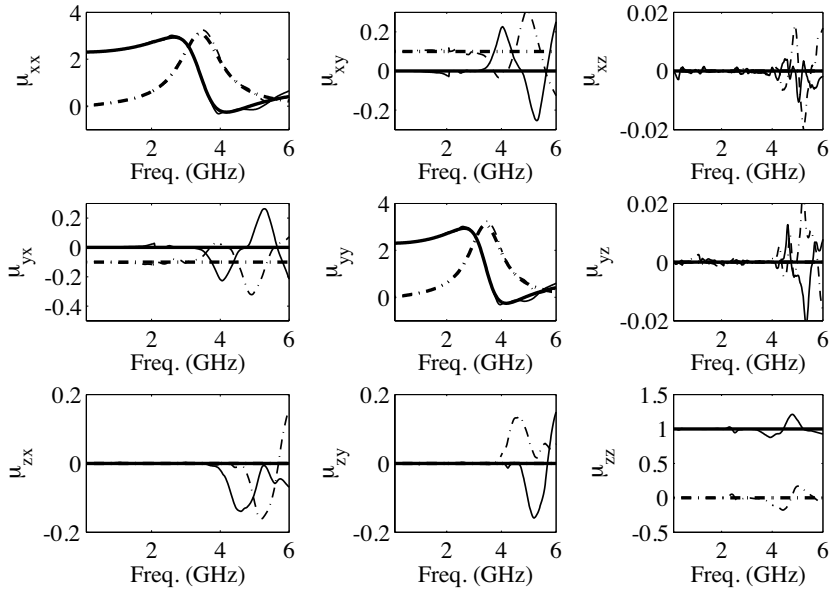

Figure 3. Comparison of the retrieved (thin lines) and the true (thick lines) $\overline{\overline{\mu}}$ of a Chiroferrite medium. The solid and dotted-dashed lines are for the real and imaginary parts, respectively.

$$\overline{\overline{\zeta}}_t = \begin{pmatrix} -9.95\times10^{-3} & -1.85\times10^{-3}-i2.54\times10^{-2} & 0 \\ 1.85\times10^{-3}+i2.54\times10^{-2} & -9.95\times10^{-3} & 0 \\ 0 & 0 & \\ & & 0 \\ & & 0 \\ & & -1.00\times10^{-2}-i5.00\times10^{-3} \end{pmatrix}.$$

Finally, for the retrieval at higher frequencies, we choose the linear extrapolation of the results at the previous two frequencies as initial guess for the simplex optimization. We observe that at 2.1 GHz, the thickness of the slab is seventy percent of the wavelength, consequently making the optimization very unstable. Thus starting at 2.1 GHz, we choose a thinner slab whose thickness is five percent of the wavelength at 2.1 GHz. The optimization results are shown in the Fig. 2–Fig. 5. The results show that most of the constitutive parameters are retrieved successfully, although there are some discrepancies around the resonant frequencies. The averaged relative mismatch of each component of the

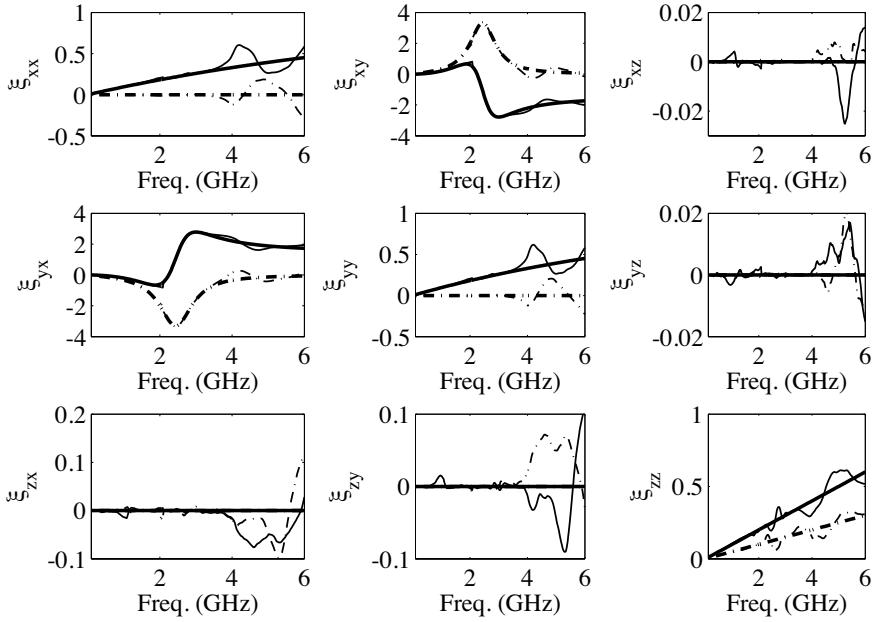

Figure 4. Comparison of the retrieved (thin lines) and the true (thick lines) $\overline{\overline{\xi}}$ of a Chiroferrite medium. The solid and dotted-dashed lines are for the real and imaginary parts, respectively.

constitutive tensors is as follows:

$$A_{RM}(\epsilon) = \begin{pmatrix} 0.113 & 0.829 & 0.003 \\ 0.810 & 0.109 & 0.004 \\ 0.028 & 0.028 & 0.064 \end{pmatrix}$$

$$A_{RM}(\mu) = \begin{pmatrix} 0.100 & 0.818 & 0.003 \\ 0.811 & 0.096 & 0.003 \\ 0.039 & 0.039 & 0.061 \end{pmatrix}$$

$$A_{RM}(\xi) = \begin{pmatrix} 0.218 & 0.078 & 0.003 \\ 0.077 & 0.212 & 0.004 \\ 0.028 & 0.026 & 0.113 \end{pmatrix}$$

$$A_{RM}(\zeta) = \begin{pmatrix} 0.254 & 0.048 & 0.003 \\ 0.047 & 0.254 & 0.003 \\ 0.041 & 0.040 & 0.076 \end{pmatrix}$$

We see that most components have an averaged relative mismatch less than 0.12.

As a second example, we consider an Omegaferrite $C_{2v}(C_s)$

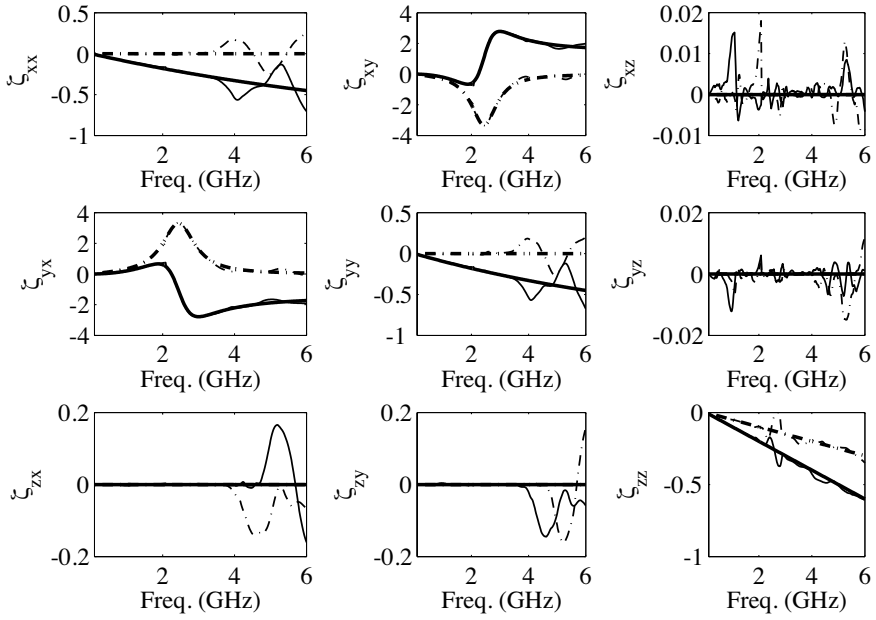

Figure 5. Comparison of the retrieved (thin lines) and the true (thick lines) $\overline{\overline{\zeta}}$ of a Chiroferrite medium. The solid and dotted-dashed lines are for the real and imaginary parts, respectively.

medium in the forward problem, whose constitutive parameters are

$$\overline{\overline{\epsilon}} = \epsilon_0 \begin{pmatrix} \epsilon_{xx} & 0 & \epsilon_{xz} \\ 0 & \epsilon_{yy} & 0 \\ -\epsilon_{xz} & 0 & \epsilon_{zz} \end{pmatrix}, \; \overline{\overline{\mu}} = \mu_0 \begin{pmatrix} \mu_{xx} & 0 & \mu_{xz} \\ 0 & \mu_{yy} & 0 \\ -\mu_{xz} & 0 & \mu_{zz} \end{pmatrix},$$

$$\overline{\overline{\xi}} = \frac{1}{c} \begin{pmatrix} 0 & \xi_{xy} & 0 \\ \xi_{yx} & 0 & \xi_{yz} \\ 0 & \xi_{zy} & 0 \end{pmatrix}, \; \overline{\overline{\zeta}} = \frac{1}{c} \begin{pmatrix} 0 & -\xi_{yx} & 0 \\ -\xi_{xy} & 0 & \xi_{zy} \\ 0 & \xi_{yz} & 0 \end{pmatrix}. \quad (17)$$

The numerical values of the constitutive parameters are chosen from [17]. In this example, we aim at testing the robustness of the linear extrapolation technique in the retrieval at the higher frequencies. Both noiseless and noisy data are tested. In the simulations, 2% and 5% Gaussian random noises are added to the reflection and transmission coefficients. The reconstruction results for noiseless and 2% noise cases, not shown here, generally match the true solutions in a similar way as shown in Fig. 2–Fig. 5 in the previous example. For the case of 5% noise, most of the constitutive parameters are also generally

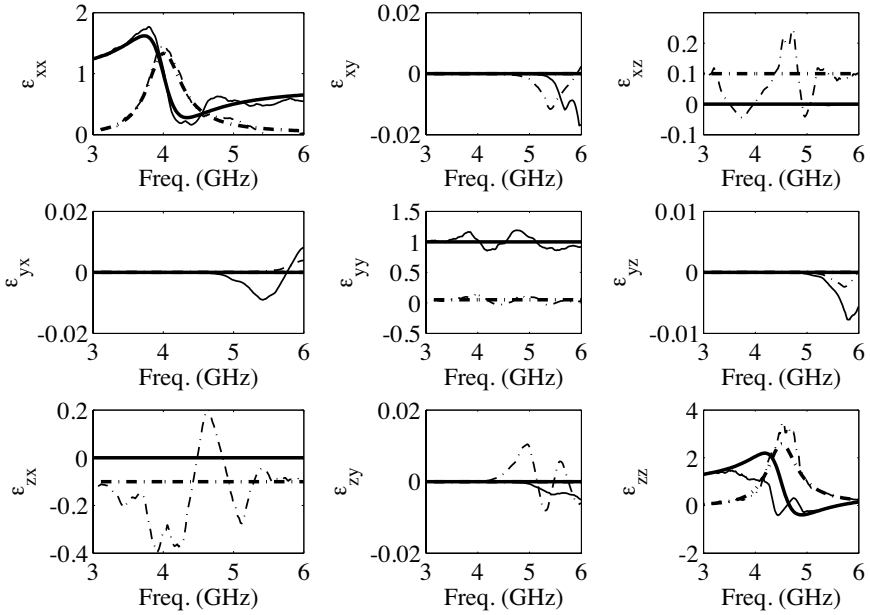

Figure 6. Comparison of the retrieved (thin lines) and the true (thick lines) $\overline{\overline{\epsilon}}$ of an Omegaferrite medium (5% noise). The solid and dotted-dashed lines are for the real and imaginary parts, respectively.

reconstructed. Most components have an averaged relative mismatch smaller than 0.25. The reconstruction results for $\overline{\overline{\epsilon}}$ are shown in the Fig. 6 for the purpose of illustration.

5. CONCLUSION

An optimization approach is used to retrieve the constitutive parameters of a slab of general bianisotropic medium from the knowledge of the reflection and transmission data. The method is for either rotated media with known constitutive properties or more general media with unknown constitutive properties. High dimensional inverse problems are tackled by the combination of the differential evolution algorithm and the simplex method. The DE is used first to parallel explore the searching space and then the simplex method is applied to accelerate the convergence. Fewer incidences are used in the DE method in order to reduce the computation burden, and diverse incidences are used in the simplex method in order to obtain the unique solution. Importantly, our method obtains a group of solutions, all

of which are almost identical to the true one. Linear extrapolation of the results at the previous two frequencies are used as an initial guess for the retrieval of dispersive medium using simplex optimization method. Both noiseless and noisy data are tested. Optimization results show that the constitutive parameters are reconstructed successfully. The limitation of the proposed method is that it cannot deal with bianisotropic media whose cross-polarization terms are not close to zero at low frequencies. However, this difficulty could be overcome by parallel computing in a reasonable time.

ACKNOWLEDGMENT

This work is sponsored by the Department of the Air Force under Air Force Contract F19628-00-C-0002, and the ONR under Contract N00014-01-1-0713. Opinions, interpretations, conclusions and recommendations are those of the author and are not necessarily endorsed by the United States Government.

REFERENCES

1. Smith, D. R. and D. Schurig, "Electromagnetic wave propagation in media with indefinite permittivity and permeability tensors," *Phys. Rev. Lett.*, Vol. 90, 077405, 2003.
2. Grzegorczyk, T. M., M. Nikku, X. Chen, B.-I. Wu, and J. A. Kong, "Refraction laws for anisotropic media and their application to left-handed metamaterials," *IEEE Trans. Microwave Theory Tech.*, Vol. 53, No. 4, 1443–1450, 2005.
3. Grzegorczyk, T. M., X. Chen, J. Pacheco, J. Chen, B.-I. Wu, and J. A. Kong, "Reflection coefficients and Goos-Hanchen shift in anisotropic and bianisotropic left-handed metamaterials," *Prog. Electromagn. Res.*, Vol. 51, 83–113, 2005.
4. Kong, J. A., *Electromagnetic Wave Theory*, EMW, Cambridge, MA, USA, 2000.
5. Kong, J. A., "Theorems of bianisotropic media," *Proc. IEEE*, Vol. 60, 1036–1046, 1972.
6. Smith, D. R., D. C. Vier, T. Koschny, and C. M. Soukoulis, "Electromagnetic parameter retrieval from inhomogeneous metamaterials," *Phys. Rev. E*, Vol. 71, 036617, Mar. 2005.
7. Chen, X., T. M. Grzegorczyk, B.-I. Wu, J. Pacheco, and J. A. Kong, "Robust method to retrieve the constitutive effective parameters of metamaterial," *Phys. Rev. E*, Vol. 70, 016608, July 2004.

8. Smith, D. R., S. Schultz, P. Markos, and C. M. Soukoulis, "Determination of effective permittivity and permeability of metamaterials from reflection and transmission coefficients," *Phys. Rev. B*, Vol. 65, 195104, 2002.
9. Chen, X., B. Wu, J. A. Kong, and T. M. Grzegorczyk, "Retrieval of the effective constitutive parameters of bianisotropic metamaterials," *Phys. Rev. E*, Vol. 71, 046610, Apr. 2005.
10. Borzdov, G. N., "Lorentz-covariant surface impedance and characteristic matrix methods with applications to measurements of material parameters of linear media," *Opt. Commun.*, Vol. 94, 159–173, 1992.
11. Borzdov, G. N., "Novel free-space techniques to characterize complex mediums," *Electromagnetic Fields in Unconventional Materials and Structures*, O. N. Singh and A. Lakhtakia (eds.), 83–124, Wiley Interscience, New York, 2000.
12. Rikte, S., G. Kristensson, and M. Andersson, "Propagation in bianisotropic media — reflection and transmission," *IEE Proc. - Microw. Antennas Propag.*, Vol. 148, 29–36, February 2001.
13. Storn, R. and K. Price, "Differential evolution — a simple and efficient heuristic for global optimization over continuous spaces," *J. Global Optim.*, Vol. 11, 341–359, 1997.
14. Nelder, J. A. and R. Mead, "A simplex method for function minimization," *Comput. J.*, Vol. 7, 308–313, 1965.
15. Tsang, L., J. A. Kong, and K. H. Ding, *Scattering of Electromagnetic Waves: Theories and Applications*, Wiley-Interscience, 2000.
16. Dmitriev, V., "Constitutive tensors of omega- and chiroferrites," *Microwave Opt. Technol. Lett.*, Vol. 29, 201–205, May 2001.
17. Chen, X., *Inverse Problems in Electromagnetics*, Ph.D. thesis, Massachusetts Institute of Technology, June 2005.